Applied Catalysis B: Environmental 164 (2015) 48–60

Contents lists available at ScienceDirect

Applied Catalysis B: Environmental

journal homepage: www.elsevier.com/locate/apcatb

A study of the hydrodenitrogenation of propylamine over supported nickel phosphide catalysts using amorphous and nanostructured silica supports

Cecília A. Badari [a], Ferenc Lónyi [a,*], Eszter Drotár [a], Alexander Kaszonyi [b], József Valyon [a]

[a] Institute of Materials and Environmental Chemistry, Research Centre for Natural Sciences, Hungarian Academy of Sciences, H-1117, Magyar tudósok körútja 2, Budapest, Hungary
[b] Department of Organic Technology, Slovak University of Technology, Radlinského 9, Bratislava SK-81237, Slovak Republic

ARTICLE INFO

Article history:
Received 11 June 2014
Received in revised form 22 August 2014
Accepted 2 September 2014
Available online 9 September 2014

Keywords:
Hydrodenitrogenation
Ni_2P/SiO_2
Ni_2P/SBA-15
Propylamine
Delplot analysis

ABSTRACT

Pyrolysis of animal by-products provides pyro-oil that contains about 10 wt% nitrogen mainly in aliphatic compounds and virtually no sulfur. The nitrogen should be removed from the oil preferably by hydrodenitrogenation (HDN) to obtain liquid fuel and ammonia. In order to understand the catalytic HDN processes of such bio-oils the HDN of propylamine (PA) was studied as model reaction over silica-supported Ni_2P and Ni catalysts. Catalysts were prepared by H_2-reduction of catalyst precursor NiO/phosphated silica gel and NiO/phosphated SBA-15 silica material and NiO/silica gel. The catalyst surface was characterized by Diffuse Reflectance Infrared Fourier Transform Spectroscopic (DRIFTS) examination of adsorbed CO. It was shown that the Ni_2P particles had a highly defected structure in the initial reduced state of the catalyst but were rapidly converted to ordered crystals in contact with PA under reaction conditions. The HDN reaction of PA was studied using a flow-through tube reactor and also by *in situ* DRIFTS experiments in the 16–60 bar pressure and 200–400 °C temperature range. Below about 300 °C the Ni_2P catalysts were active in the direct hydrogenolysis of the C—N bond of PA, however, the main reaction was the PA disproportionation to dipropylamine (DPA) and ammonia. Above about 300 °C the hydrogenolysis of the DPA C—N bond became the main reaction. Near to full HDN of PA could be attained without hydrogenolysis of C—C bond. In contrast, Ni/silica gel catalyst was hardly active in the direct C–N hydrogenolysis of PA but was active in the PA disproportionation to DPA. Above about 300 °C reaction temperature ammonia, less propane, and significant amount of methane and ethane were formed.

1. Introduction

Numerous studies have been devoted to the deeper understanding of the catalytic hydrogenation reactions of N-containing organic compounds to support the improvement of hydrodenitrogenation (HDN) technology of petroleum industry [1–3]. The HDN of aromatic molecules was found to begin with full saturation of the N-containing aromatic ring and the formation of primary amine by breaking one C—N bond. The hydrodenitrogenation of nitriles is introduced also by formation of alkylamines. Because mineral oil fractions usually contain also sulfur-compounds the reactions of HDN and hydrodesulfurization (HDS) proceed together. The N-compounds are inhibitors of the HDS reaction, therefore most studies concern the HDN of model compounds over supported or non-supported transition metal sulfides or phosphides in the presence of sulfur compound in the feed. The ammonia was substantiated to be released from quaternized ammonium compound, formed by protonation of the primary amine, on the attack of a nucleophilic HS^- or S^- species on the catalyst surface [1].

Nowadays more and more attention is focused on the conversion of waste biomass to more favorable energy carrier and energy. Beside the abundantly available lignocellulosic waste materials [4], animal by-products [5], such as meat and bone meal (MBM) represent significant chemical energy and a potential liquid fuel and N-fertilizer resource. Pyrolysis converts a large fraction of the biomass to oily liquid. The pyro-oil gained from animal by-products contains about 10 wt% nitrogen mainly in aliphatic compounds, 5 wt% oxygen and virtually no sulfur [5–7]. By catalytic hydroprocessing of the oil valuable products, preferably hydrocarbons and

* Corresponding author. Tel.: +36 1 382 6864.
E-mail address: lonyi.ferenc@ttk.mta.hu (F. Lónyi).

http://dx.doi.org/10.1016/j.apcatb.2014.09.001
0926-3373/

ammonia are expected to be obtained. The hydrocarbon product can be used as environmental-friendly, carbon dioxide neutral fuel. By converting the ammonia to N-fertilizer, the nitrogen-content of the waste can be recycled to the agriculture. It is a further environmental benefit that the hazardous waste animal by-product is disposed.

The HDN of sulfur-free reaction mixture over nickel phosphide catalyst (Ni_2P/SiO_2) was hardly studied before. The present work concerns the HDN of 1-propylamine (PA) over Ni_2P/SiO_2 in a broad pressure and temperature range with the objective to gain better understanding of the reaction mechanism and to provide better scientific bases to the hydroprocessing technology of low sulfur or sulfur-free feeds, rich in organic N-compounds.

2. Experimental

2.1. Catalyst preparation

Nickel phosphide catalysts supported on silica gel (SYLOBEAD B127, Grace Davison; specific surface area: 563 m^2/g) or silica material SBA-15 (our synthetic product, synthesized from sodium silicate using a triblock copolymer P123 as template; specific surface area: 800 m^2/g) were prepared by incipient wetness impregnation followed by calcination and controlled reduction of the nickel phosphide precursor compound according to refs. [2,3]. The impregnating solution was prepared by dissolving 3.04 g (23.0 mmol) of $(NH_4)_2HPO_4$ (Fluka, +99%) in 5.0 cm^3 distilled water and adding 3.36 g (11.56 mmol) of $Ni(NO_3)_2$ (Merck, +99%) to the solution (initial P/Ni molar ratio of 2). A precipitate was formed. Concentrated cc. HNO_3 solution was added dropwise to the mixture until the precipitate was fully dissolved and a transparent green solution was obtained. This solution was then used to impregnate 10 g of the support previously dried at 120 °C overnight. The impregnated support was dried at 120 °C for 6 h and then calcined at 400 °C for 4 h. Formation of nickel phosphide was effected by treating the samples in 100 $cm^3\ min^{-1}$ H_2 flow at elevated temperature. The temperature of the samples was raised at a rate of 2 °C min^{-1}. The silica gel and the silica SBA-15 supported catalysts were reduced at 650 °C and 700 °C, respectively, for 3-3 h. The reduction temperatures were chosen based on results of the temperature-programmed reduction (H_2-TPR) and *in situ* high-temperature X-ray diffraction measurements. Finally, the sample was cooled to room temperature in He flow (20 $cm^3\ min^{-1}$) and then contacted with a 50 $cm^3\ min^{-1}$ flow of 1.0% O_2/He for 4 h. Latter treatment aimed to passivate the pyrophoric Ni_2P particles by generating phosphate-like surface layer that prevents the bulk of the particle to become oxidized when the sample is exposed to air [8–10]. When the obtained material is to be used as catalyst it has to go first through an activating treatment in H_2 flow at 450 °C. The catalyst samples are designated as Ni_2P/SiO_2 and Ni_2P/SBA-15. Further on the attribute "passivated" or "activated" or "used" is added to the sample name to refer to the last pretreatment of the preparation that determines the nature of its surface.

For comparative purposes phosphated silica (PO_x/SiO_2) and silica supported Ni catalyst were also prepared. The PO_x/SiO_2 was prepared by impregnating the silica gel support with the same amount of $(NH_4)_2HPO_4$ than that used for the preparation of Ni_2P/SiO_2, however without adding the Ni precursor to the impregnating solution. The impregnated support was dried at 120 °C for 6 h and then calcined at 450 °C for 4 h. The Ni/SiO_2 catalyst was prepared similarly as silica supported Ni_2P catalysts, but without adding $(NH_4)_2HPO_4$ to the impregnating solution. The impregnated support was dried at 120 °C for 6 h and then calcined at 450 °C for 4 h and finally reduced in H_2 flow at 500 °C for 3 h.

2.2. Catalyst characterization

2.2.1. X-ray powder diffraction (XRD)

XRD patterns of the samples were obtained with a Philips PW 1810 powder diffractometer, equipped with a graphite monochromator, using Cu Kα radiation (λ = 0.15418 nm) and proportional counter. The X-ray tube was set at 40 kV and 35 mA. The step width of scan was 0.04° and, in each step, the counts were digitally recorded. *In situ* X-ray diffraction measurements were carried out using a type HT1200 Anton Paar chamber in order to study the reduction process of the calcined catalyst precursors, i.e. to follow the formation of the active nickel phosphide phase. The samples were heated in H_2 flow from room temperature up to 650 °C at a heating rate of 10 °C min^{-1}. The temperature program was stopped at 450, 500, 550, 600, and 650 °C for 30 min. The XRD patterns were recorded after 30 min treatment in H_2 flow at these temperatures. The temperature of H_2 treatment required to get activated catalysts was selected on the bases of these *in situ* high-temperature X-ray diffraction measurements and the H_2-TPR pattern of the catalyst precursors (see below). XRD patterns of the catalyst samples activated at the selected temperatures were also measured at room temperature. Crystallite sizes were determined from line broadening using the Scherrer equation.

2.2.2. Chemical composition

The nickel and phosphorous content of the as-prepared Ni_2P/SiO_2 and Ni_2P/SBA-15 catalysts was determined by ICP-OES analysis.

2.2.3. Specific surface area

The specific surface area of the samples was calculated from isotherms of nitrogen adsorption at 77 K using the BET method. The isotherms were measured by Quantachrome NOVA Automated Gas Sorption Instrument. The samples were evacuated at 350 °C for 1 h before the measurements.

2.2.4. Transmission electron microscopy (TEM)

Diluted suspensions of samples in methanol were prepared and drop-dried on carbon coated copper TEM grids. TEM images were taken by type Morgagni 268D microscope (100 kV, W filament, point-resolution = 0.5 nm).

2.2.5. Temperature-programmed reduction by hydrogen (H_2-TPR)

H_2-TPR was used to determine the reduction temperature required to convert the calcined catalyst precursor to supported nickel phosphide catalyst. The reduction of the catalyst precursors was carried out in a U-shaped quartz tube reactor having an internal diameter of 6 mm. The reactor was placed in a furnace controlled by temperature programmer. The catalyst samples were heated up to 400 °C at a rate of 10 °C min^{-1} in nitrogen flow of 30 $cm^3\ min^{-1}$, kept at this temperature for 1 h, then cooled to room temperature in nitrogen. The TPR experiment was carried out by changing the N_2 flow to a 30 $cm^3\ min^{-1}$ flow of 10% H_2/N_2. The effluent gas was passed through a dry-ice trap and a thermal conductivity detector (TCD). Data were collected and processed by computer. According to earlier studies treatment temperatures, higher than that required to generate Ni_2P phase, was found to result in lowered Ni_2P dispersion and, as a consequence, in lower hydroconversion activity [11,12]. The TPR results were used to determine the preferable lowest temperature of precursor-to-catalyst conversion and also the H_2 demand of the process.

2.2.6. Temperature-programmed H_2 desorption (H_2-TPD)

The H_2-TPD measurements were carried out on the same instrument that was used for H_2-TPR measurements. The passivated

catalysts were activated in flowing H_2 (30 cm^3 min^{-1}) in the reactor tube for 1 h. The pretreatment temperature was 550 °C for Ni_2P samples and 450 °C for Ni/SiO_2 sample. After reduction the sample was allowed to cool to room temperature in H_2. The TPD experiment was carried out by changing the H_2 flow to a 30 cm^3 min^{-1} flow of N_2. The catalyst samples were heated up to 600 °C at a rate of 10 °C min^{-1} in the N_2 flow and kept at this temperature for 1 h. The reactor effluent was passed through a dry-ice trap and a thermal conductivity detector (TCD). The amount of desorbed H_2 was calculated from the integrated area of the TPD curve. The Ni dispersion in the Ni/SiO_2 catalyst was calculated according to Subramani et al. [13] as the molar ratio of the Ni on the surface of the particles to the total Ni content. The same method was applied to estimate the dispersion of the supported Ni_2P phase. The amount of surface Ni atoms was considered as equivalent with the amount of H-atoms in the desorbed H_2 gas.

2.2.7. DRIFTS examination of CO chemisorption

Carbonyl species obtained from the adsorption of CO on the catalyst was studied by DRIFT spectroscopy using a Nicolet 5PC spectrometer equipped with a COLLECTOR™ diffuse reflectance mirror system and a flow-through DRIFT spectroscopic reactor cell (Spectra-Tech, Inc.). The sample cup of the cell was filled with about 20 mg of powdered catalyst sample. The catalyst was reduced first in H_2 flow at 550 °C for 1 h then was purged with He at 550 °C for 1 h, cooled to room temperature and the spectrum of the activated catalyst powder was taken. This spectrum was subtracted from the spectra collected after contacting the sample with a flow of 3% CO/He at room temperature to get characteristic difference spectra. Note that these latter spectra were corrected with the spectrum of gas phase CO in order to remove its contribution from the spectra and thus obtain the spectra of adsorbed CO only. Spectra were taken also after purging the cell with He at room temperature and at 100, 200 and 300 °C for 10 min at each temperature.

2.3. Catalytic activity

The 0.315–0.63 mm sieve fraction of catalyst particles was filled in a flow-through stainless steel tube microreactor to study the catalytic hydroconversion of PA (Alfa Aesar, 99+%). The PA was fed into the reactor by a high-pressure liquid pump. The hydrogen flow rate and pressure were controlled by electronic mass flow controller (Brooks Instrument Ltd., Hungary) and a back pressure regulator, respectively. The reactor effluent line together with the back pressure regulator and sampling valve were kept at 150 °C in order to avoid condensation in the system. Catalysts were activated in a 100 cm^3 min^{-1} hydrogen flow at 450 °C for 1 h. The reaction temperature was varied in the range of 200–400 °C at 30 bar total pressure, and at a H_2/PA molar ratio of 10. The weight hourly space velocity (WHSV) of the reactant PA was varied between 0.75 and 3.0 h^{-1}. When the effect of hydrogen partial pressure was studied the H_2/PA molar ratio and the total pressure was changed between 5–20 and 16.2–56.7 bar, respectively. Each catalyst samples were tested for about two weeks, while several measurements at a given set of parameters were repeated in order to check the stability of the catalysts. All the catalysts showed stable activity during this time period. No coke deposition was perceptible to the eye on the catalysts removed from the reactor. The carbon content of the feed and the products was virtually equal. The composition of the reactor effluent was analyzed using on-line a Shimadzu GC-2010Plus type gas chromatograph, equipped with a flame ionization detector and a Supelco EQUITY-1 type capillary column. The main products of the reaction were ammonia, dipropylamine (DPA) and tripropylamine (TPA), propane and, in some experiments, some other lower alkanes. The PA conversion and the NH_3 yield were calculated as follows:

$$\text{Conversion, } \% = \left(\frac{[\text{Propane}] + 2[\text{DPA}] + 3[\text{TPA}]}{[\text{PA}] + [\text{Propane}] + 2[\text{DPA}] + 3[\text{TPA}]}\right) \times 100,$$

$$\text{Yield of } NH_3, \% = [\text{Propane}] + [\text{DPA}] + 2[\text{TPA}],$$

where the symbols in brackets stand for the molar concentration of the corresponding compounds. The correctness of the calculated ammonia yield was checked by measuring the NH_3 concentration in the reactor effluent. The calculated and the measured data showed only scarce deviation, therefore, the NH_3 yield was routinely determined by calculation.

2.4. DRIFT spectroscopic examination of the HDN reaction

The spectral analysis of the catalyst surface during catalytic HDN of PA was studied using the same DRIFTS apparatus as the one used for the above described CO chemisorption studies. First the catalyst was treated *in situ* in the DRIFTS reactor cell in a 30 cm^3 min^{-1} flow of H_2 at 550 °C for 1 h in order to remove the passivating phosphate surface layer of the nickel phosphide particles. On each temperature whereon we run *in situ* catalytic tests in the DRIFTS cell the spectrum of the catalyst powder was recorded in H_2 flow. The reaction was initiated by switching the H_2 flow to a gas saturator containing PA at 0 °C and thus setting 0.14 bar partial pressure of amine in the reaction mixture. The total pressure in the reactor cell was raised from atmospheric to 20 bar using a back pressure regulator upstream the cell. Spectra were then taken at temperatures between 100 and 400 °C. The spectrum obtained from the catalyst and the reacting gas was corrected with the spectrum of the catalyst in H_2 at the reaction temperature. The result is a difference spectrum showing the bands of surface species and the absorption bands coming from the vibration–rotation modes of molecules in the gas above the operating catalyst.

3. Results

3.1. XRD and H_2-TPR results

The H_2-TPR curves of the catalyst precursors and the powder XRD patterns of the catalysts obtained by reducing the precursors are given in Fig. 1. The temperature of H_2, treatment required to get activated catalyst, was selected on the bases of the H_2-TPR pattern of the catalyst precursors and results of *in situ* high-temperature X-ray diffraction measurements (not shown). It was clearly shown that the Ni_2P phase appears at treatment temperature, whereon H_2 consumption indicates reduction of the precursor compounds on the surface of the silica support. The selected reduction temperature was 500 °C to get Ni/SiO_2, whereas 650 and 700 °C to obtain Ni_2P/SiO_2 and Ni_2P/SBA-15 catalysts, respectively (Fig. 1). The diffraction patterns of the catalysts (Fig. 1B) show diffraction lines located at 2Θ degrees of 40.7°, 44.5°, 47.3° and 54.2°, identifying Ni_2P phase (ICDD card No.: 03-0953). The diffraction lines of the Ni_2P phase on the higher surface area SBA-15 support are broader, than the corresponding lines of this phase on silica. The reflections of Ni/SiO_2 (Fig. 1B) at 2Θ degrees of 44.5° and 51.8° is ascribed to the presence of Ni^0 (ICDD card No.: 04-0852). The broad reflection at about 2Θ degrees 15–30° is coming from the amorphous silica support.

The average size of the supported particles, given in Table 1, was calculated by the Scherrer equation using the main diffraction lines of the Ni_2P and Ni phases at 40.7° and 44.5°, respectively. Data suggest that the mesoporous silica SBA-15 support favors more the formation of highly dispersed Ni_2P than the microporous silica gel support. The XRD results and the TEM pictures show that

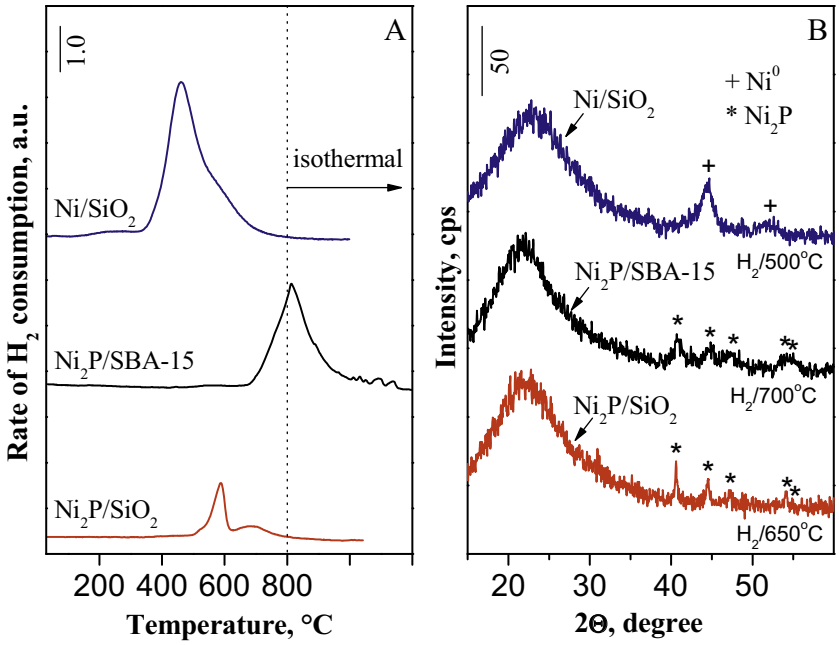

Fig. 1. (A) H_2-TPR curves measured over the catalyst precursors of Ni/SiO_2, $Ni_2P/SBA-15$, and Ni_2P/SiO_2 catalysts, and (B) XRD patterns of the corresponding catalyst samples reduced in H_2 at the indicated temperature for 3 h.

Table 1
Characterization of catalysts.

Catalysts	SSA[a] (m^2/g)	Ni (wt%)	P (wt%)	Dispersion[b] (%)	D^c (nm)	D^d (nm)
Ni_2P/SiO_2	268 (563)	5.04	4.11	15.4 (41.4)	20–60	49 (55)
$Ni_2P/SBA-15$	162 (800)	7.32	4.07	34.8 (114.2)	5–15	10 (10)
Ni/SiO_2	558 (563)	6.76	–	9.2 (28.8)	2–10	11

[a] SSA = specific surface area, determined by the Brunauer-Emmett-Teller (BET) method (specific surface area of the support is given in parentheses).
[b] Dispersion of particles determined from H_2-TPD measurements. The amount of H_2 evolved (μmol H_2/g_{cat}) is given in parenthesis.
[c] Diameter of particles of the active phase observed in the TEM micrograph.
[d] Particle size calculated from XRD by Scherrer equation (particle size for used catalyst is given in parentheses).

the Ni^0 particles in the Ni/SiO_2 catalyst are the smallest (Table 1, Fig. S1). The XRD pattern of the $Ni_2P/SBA-15$ catalyst, used in the catalytic PA HDN reaction (not shown), was similar to that of the fresh catalyst, demonstrating that the Ni_2P morphology was stable under hydrotreating conditions. In contrast, the used Ni_2P/SiO_2 catalyst present more intense diffraction peaks, suggesting that the Ni_2P assembled is more ordered crystalline phase than it was in the activated fresh catalyst (Table 1).

It is known that nickel metal easily forms tetracarbonyl and subcarbonyls. Therefore, the determination of Ni dispersion from the CO chemisorption uptake of the Ni catalysts is not suggested. The nickel dispersion (Table 1) was calculated, therefore, from the amount of chemisorbed H_2, determined by H_2-TPD (Fig. S2). The average Ni^0 particle size corresponding to the obtained dispersion was 10.8 nm that was in good agreement with the average particle size obtained from the XRD result and the size of the Ni^0 particles observed on the TEM pictures. Earlier studies [14–16] used the CO chemisorptions method to determine the Ni_2P dispersion of supported nickel phosphide catalysts. In the present study we attempted to use the H_2 chemisorption method to estimate the Ni_2P dispersion of our catalysts. Interestingly, much higher dispersions were obtained than for the Ni^0. These high dispersions are in obvious contradiction with the average Ni_2P particle size, obtained from the XRD result and observed on the TEM pictures, which are much larger than that of the Ni^0 particles in the Ni/SiO_2 catalyst (Table 1, Fig. 2 and Fig. S1). The contradictory results may indicate that the amount of desorbed H-atoms exceeds the number of surface Ni atoms. It is well known that not only metal atoms can release hydrogen but also surface hydroxyl groups, participating in redox reaction with the supported metal [17] or other surface species. These results suggest that not only the CO but also the H_2 chemisorption method must be used with extreme caution for the determination of active phase dispersion over oxide support.

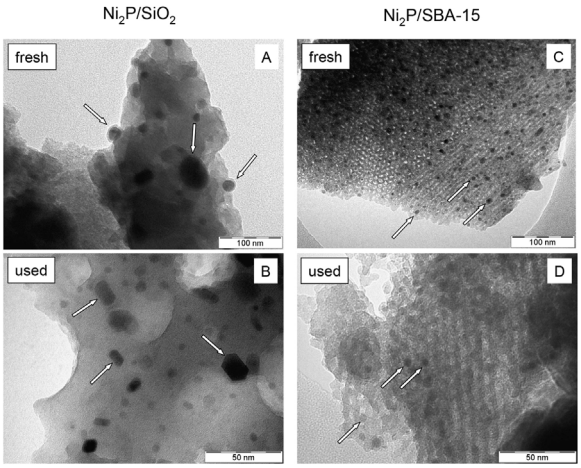

Fig. 2. TEM micrographs of fresh and used (A,B) Ni_2P/SiO_2 and (C,D) $Ni_2P/SBA-15$ catalysts.

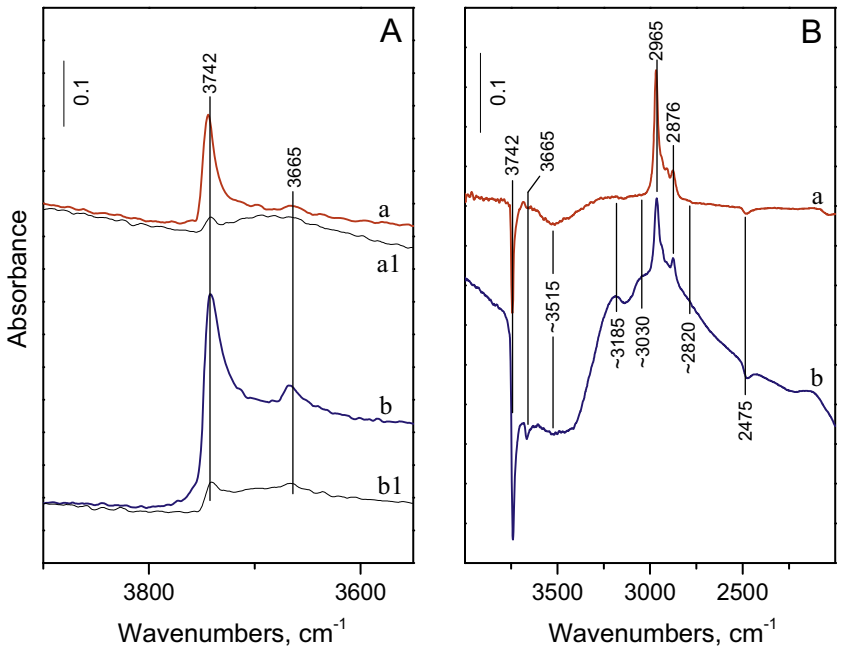

Fig. 3. DRIFT spectra of the (A) ν_{OH} region of the (a) fresh and (a1) used Ni_2P/SiO_2 catalyst. Spectra b and b1 are the corresponding spectra of the Ni_2P/SBA-15 catalyst. Before spectra were recorded at room temperature the samples were pretreated *in situ* in the DRIFTS cell in H_2 flow at 550 °C for 1 h then was purged with He at 550 °C for 1 h. Section B shows the difference of the spectra of fresh and used (a) Ni_2P/SiO_2 and (b) Ni_2P/SBA-15 catalyst.

3.2. DRIFT spectra of the samples and of adsorbed CO

Fig. 3A shows that the OH-bands of the used catalysts are significantly weaker than those of the activated ones suggesting that adsorbed species consumed OH groups or perturbed ν(OH) vibration. To shed light on the nature of the adsorbed species difference spectra were generated by subtracting the spectrum of the activated catalyst from that of the corresponding used one (Fig. 3B). The relatively broad positive bands at ~3185, 3030, and 2820 cm^{-1} are due to ν_{NH} vibrations. These bands closely remind of those obtained from adsorption of ammonia on H-zeolites [18] or on Brønsted acid P-OH sites of phosphated silica [19,20]. The bands are assigned to species formed by protonation of ammonia, product of the HDN reaction, or to protonated alkyl amines. The negative ν(OH(P)) band at 3665 cm^{-1} clearly shows the involvement of the P-OH sites in the interaction with the N-bases. The adsorption affects also other P-OH vibrations, for instance the first overtone of the ν_s(P-O(H)) vibration that results in the appearance of a negative band at 2475 cm^{-1} [19]. The band at 3742 and the broad band at ~3515 cm^{-1} stem from vibration of free (terminal) Si-OH groups, and from Si-OH groups, H-bonding to each other, respectively (Fig. 3A). The corresponding negative bands in Fig. 3B suggest that silanol groups were also affected, although silanol hydroxyls cannot protonate ammonia. Therefore, the silanols were either lost by dehydroxylation or the ν(OH) frequency was shifted by H-bonding interaction with adsorbed species. The absorption bands in the range of 2970–2870 cm^{-1} are assigned to ν(CH) vibrations of alkyl groups of strongly adsorbed species. Note that not the surface of the active Ni_2P phase was covered by these species since the strength of the carbonyl bands of the activated and the used catalysts was roughly the same (Fig. 4A,B and C,D).

The spectrum of the phosphated silica (PO_x/SiO_2) sample, treated in He flow at 450 °C, presents sharp bands at 3742 and 3665 cm^{-1} (Fig. 5, a), which were assigned to ν(OH) vibrations of free Si-OH and P-OH groups, respectively [19]. The P-OH groups belong to hydrogen phosphate species, bound to silica by ester bonds, like $(SiO)_2P{=}O(OH)$. In the spectrum of the Ni_2P/SiO_2 preparations ν(OH) bands appeared at about the same frequencies (Fig. 5, b,c). Before the spectrum of the passivated Ni_2P/SiO_2 (Fig. 5, b) was recorded it was treated at 550 °C in He flow. The DRIFT spectrum of the catalyst H_2-activated at the same temperature is given in Fig. 5, c. The difference in the pre-treatment temperature of the Ni_2P/SiO_2 and the PO_x/SiO_2 preparations explains the found difference in the OH band intensities of the samples. Interestingly, the passivated and the activated catalysts show P-OH band of about the same strength. This result suggests that the amount of P-OH groups over the passivated Ni_2P particles, if any, is negligible relative to the total P-OH concentration of the catalyst sample. The high P-OH concentration is a consequence of the application of phosphate in large stoichiometric excess to nickel in the process of Ni_2P generation [21].

Fig. 4A and B shows the DRIFT spectra of the carbonyl species obtained from adsorption of CO on the surface of passivated Ni_2P/SiO_2 (Fig. 4A, a1) and activated (H_2-reduced) Ni_2P/SiO_2 catalysts (Fig. 4A, a–e), and on the surface of the Ni_2P/SiO_2 catalyst used prior to the spectroscopic examination in the catalytic HDN reaction of PA (Fig. 4B, a-e). Similar characterization is shown for activated and used Ni_2P/SBA-15 in Fig. 4C and D, respectively.

In the spectra obtained for the Ni_2P/SiO_2 catalyst, being in contact with a flow of atmospheric 3% CO/He gas, carbonyl band appeared at 2195 cm^{-1} (Fig. 4A, a1,a). In the spectrum of the passivated catalyst (Fig. 4A, a1) this was the only band, whereas bands of other carbonyls also appeared in that of the pre-reduced catalyst (Fig. 4A, a). Flushing the cell by He flow eliminated the 2195 cm^{-1} band, suggesting that it came from CO weakly bound to the surface via electrostatic interaction and/or weak σ bond [22,23].

Adsorption of CO on the Ni/SiO_2 reference catalyst gave characteristic bands (not shown) at 2070 cm^{-1} with a shoulder around 2030 cm^{-1}, and a band at 1925 cm^{-1} assigned to the ν(CO) vibration of carbonyl groups linearly bound to one Ni atom and adsorbed bridging between two neighboring surface Ni atoms, respectively. From adsorption of CO over activated Ni_2P/SiO_2 catalyst carbonyl bands were obtained at 2096, ~2055 and 2035 cm^{-1} (Fig. 4A, a). These bands are assigned to carbonyls linearly bound to Ni_2P [21,22,24]. The carbonyls over the Ni_2P/SiO_2 are similar to those, which were found over silica supported Ni catalysts [23,25] but

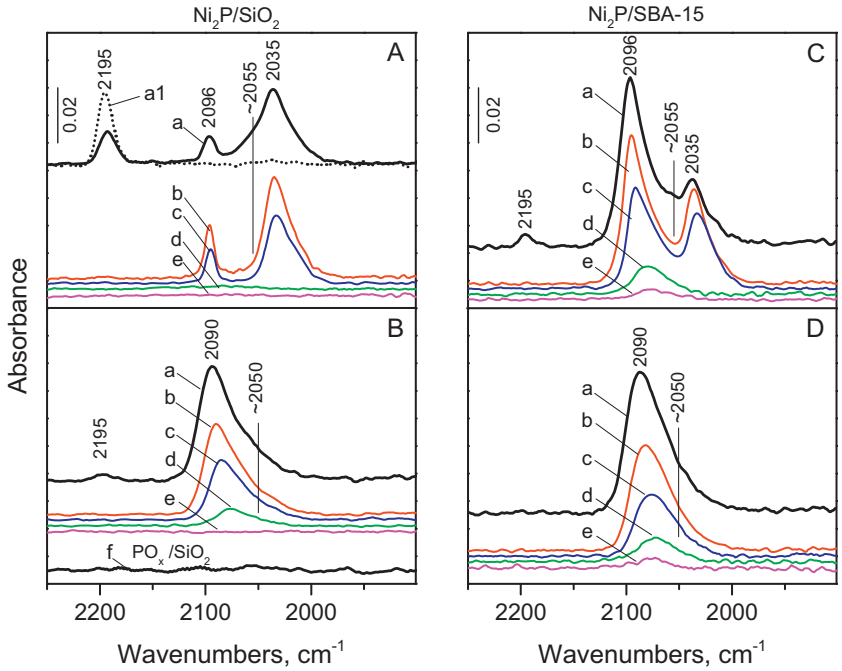

Fig. 4. DRIFT spectra of adsorbed CO on (A,B) Ni_2P/SiO_2 and (C,D) Ni_2P/SBA-15 catalysts. Spectra were taken either on the fresh (A,C) or used (B,D) catalyst samples at room temperature in the presence of gas phase CO in the IR cell (spectra a, a1 and f) and after purging the DRIFTS cell with He at room temperature (spectra b), 100 °C (spectra c), 200 °C (spectra d), and 300 °C (spectra e) for 10 min at each temperature. Spectrum (a1) was measured over the passivated Ni_2P/SiO_2 catalyst, whereas spectrum (f) was collected on the phosphated silica (PO_x/SiO_2) reference sample. Before spectra were recorded at room temperature the samples were pretreated *in situ* in the DRIFTS cell in H_2 flow at 550 °C for 1 h then was purged with He at 550 °C for 1 h.

appear at somewhat higher wavenumbers. No carbonyl band was detected below about 2000 cm^{-1} that would indicate formation of bridging carbonyl groups.

Based on the work of Morandi et al. [26] the bands at 2096 and 2035 cm^{-1} are assigned here to CO adsorbed on terrace atoms of crystal faces and on high-energy defect sites, respectively. Interestingly, the band at 2090 cm^{-1} becomes the dominating carbonyl band of the used Ni_2P/SiO_2 catalyst (Fig. 4B, a–e) suggesting that the Ni_2P phase was re-structured under reaction conditions and took on a less defected structure. The TEM pictures of the fresh and used Ni_2P/SiO_2 catalyst samples visualize above mentioned structural change (Fig. 2A,B). The fresh catalyst contains round-shape, probably partially amorphous Ni_2P particles, whereas the particles of the used catalyst look like crystals terminated by well-formed flat low energy facets. The average size of Ni_2P particles seems to be the same in both the activated and the used catalysts suggesting that mainly re-structuring of the Ni_2P particles occurred during the catalytic reaction and not much sintering. The carbonyl band at 2090 cm^{-1} is the dominating band if the Ni_2P crystals on the TEM picture show flat terminating facets, suggesting that the band belongs to CO adsorbed on mentioned crystal faces. The broadening of the band at the low frequency side (a shoulder around 2050 cm^{-1}) is probably due to CO adsorption on the higher index crystal faces.

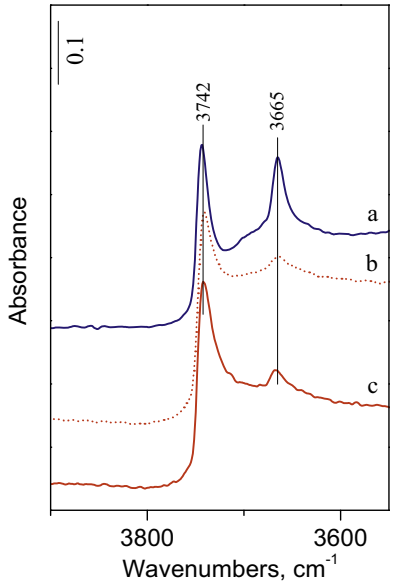

Fig. 5. DRIFT spectra of the ν_{OH} region of (a) phosphated silica (PO_x/SiO_2) sample, and (b) passivated Ni_2P/SiO_2 catalyst (dotted curve) after *in situ* treatment in He flow at 550 °C, and (c) Ni_2P/SiO_2 catalyst, after activation *in situ* in the DRIFTS cell in H_2 flow at 550 °C.

The CO spectrum of the activated Ni_2P/SBA-15 catalyst shows much similarity to the CO spectrum of the used than to the activated Ni_2P/SiO_2 (cf. Fig. 4A,a; B,a and C,a). The carbonyl band at 2096 cm^{-1} is very strong, whereas the 2195 cm^{-1} band of the Ni^{2+}-CO species is weak (Fig. 4C,a). Notice that the SBA-15 supported catalyst precursor was reduced at higher temperature than SiO_2 supported preparation to generate Ni_2P phase. This may explain the found morphological differences of the activated catalysts.

3.3. Propylamine hydrodenitrogenation

In Fig. 6, PA hydroconversion and selectivity is shown over silica supported Ni and Ni_2P catalysts as a function of the reaction temperature. The products of PA HDN are propane and ammonia. DPA and TPA appeared as by-products in concentration that depended on the reaction conditions and the activity of the catalyst (Fig. 6A–C). The direct C—N bond hydrogenolysis of PA gives equivalent amount of ammonia and propane. However, no propane but ammonia is formed in the conversion of PA to DPA and TPA. In contrast, no ammonia but propane is formed by the C—N bond

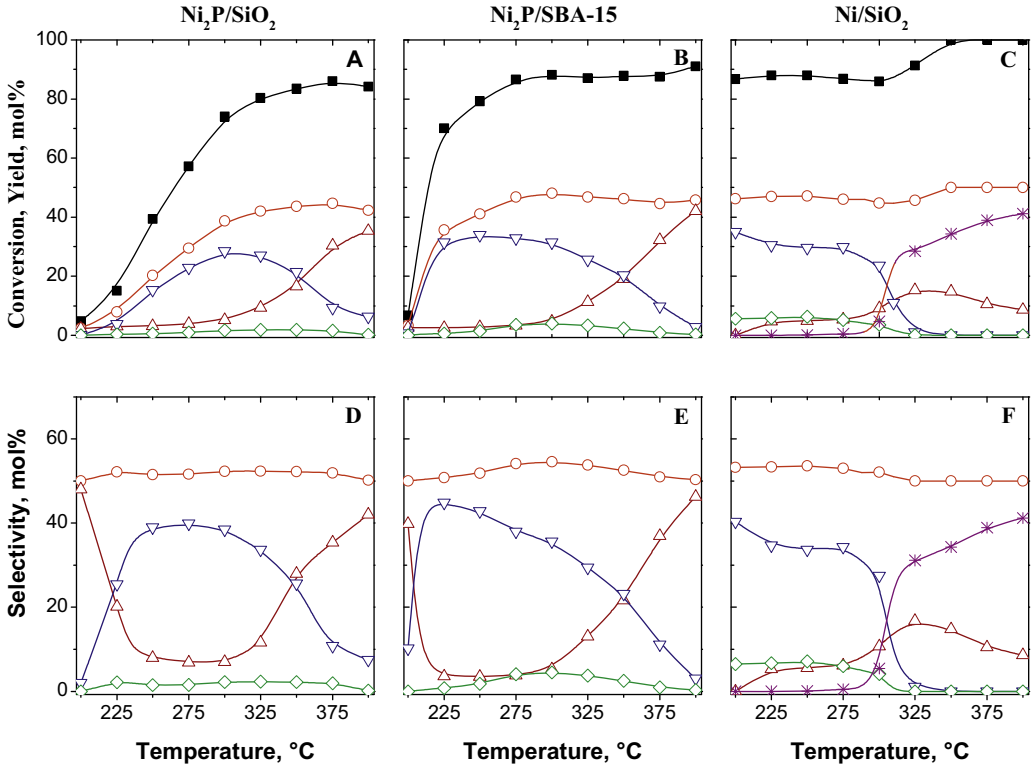

Fig. 6. Yields and selectivities of PA hydroconversion over (A,D) Ni_2P/SiO_2, (B,F) Ni_2P/SBA-15, and (C,F) Ni/SiO_2 catalysts as a function of reaction temperature. Conversion of PA (■) and yield and selectivity values for the ammonia (○), propane (△), DPA (▽), TPA (◊), and C1–C2 hydrocarbon (*) products were measured at H_2 partial pressure of 27.3 bar, PA partial pressure of 2.7 bar and at WHSV of 1 $g_{PA}\ g_{cat}^{-1}\ h^{-1}$.

hydrogenolysis of DPA and TPA beside primary or secondary amine, respectively. One objective of the present study is to understand and describe the reaction network of the PA HDN reaction.

The reference catalyst Ni/SiO_2 was very active in the PA hydroconversion. About 80% conversion was attained at temperature as low as 200 °C. The main reaction was the PA disproportionation to DPA and ammonia. Small amount of TPA was also formed (Fig. 6C,F). The virtual absence of propane in the product mixture at this low reaction temperature indicates that the catalyst is hardly active in the direct C–N hydrogenolysis of PA. Above about 300 °C reaction temperature ammonia, less propane, and significant amount of methane and ethane were obtained. This is not surprising because supported Ni catalysts are known about their high activity in C—C bond hydrogenolysis.

The silica supported Ni_2P catalysts were less active in the PA conversion than the reference catalyst Ni/SiO_2. The conversion, attained over the Ni catalyst already at 200 °C, was reached at 275 °C over Ni_2P/SBA-15 and only at 350 °C over Ni_2P/SiO_2 catalyst (Fig. 6A–C). However, significant selectivity to propane and ammonia was observed already at low temperature, showing that the Ni_2P catalysts are active in the C–N hydrogenolysis (Fig. 6D,E). At higher temperatures the PA disproportionation became the main reaction as shown by the high DPA and reduced propane selectivity (Fig. 6D,E). Above about 300 °C the C—N bond hydrogenolysis speeded up again. Propane and ammonia became the main products. It is to be noticed that nearly full HDN of PA could be attained using silica-supported Ni_2P catalysts while C–C hydrogenolysis did not occur at all.

The effect of H_2 partial pressure on PA hydroconversion over Ni_2P/SiO_2 catalyst is demonstrated by Fig. 7. The propane yield was hardly affected by the increased H_2 pressures at low temperatures. However, at temperatures where mainly the DPA and TPA products were further converted the higher H_2 pressures suppressed the conversion of DPA and, thereby the total PA conversion. As a result the DPA yield and selectivity stabilized at a higher level on expense of a lower propane yield and selectivity (Fig. 7).

3.4. *In situ DRIFT spectroscopy*

Difference infrared spectra of species, obtained by subtracting the spectrum of the catalyst from the more complex spectrum of the catalyst and the reacting PA/H_2 mixture are presented in Figs. 8 and 9. Because the spectral features and their responses to changed reaction conditions were very similar for catalysts Ni_2P/SiO_2 and Ni_2P/SBA-15, the results obtained for the Ni_2P/SiO_2 catalyst is discussed here in more details.

Involvement of hydroxyl groups in H-bonding interaction generally induces bathochromic shift of the ν_{OH} frequency. In the difference spectrum the shift generate negative band at the original position of the ν(OH) band and broad more intense positive band(s) at lower wavenumbers. The appearance of negative ν_{OH} bands in the difference spectrum indicates that surface hydroxyl groups of the catalyst are consumed or perturbed by adsorption interaction with reactant or product molecules. The appearance of positive bands unequivocally shows formation of a new species. Negative bands in the ν(OH) region appeared at 3740, 3665, and ~3520 cm^{-1}. The band at 3740 cm^{-1} and the broad band at about 3520 cm^{-1} (not labeled on the spectra) are assigned to free and associated silanol groups, respectively, suggesting that molecules from the reacting mixture interact with the Si-OH groups via hydrogen bonding. H-bonding with the strong nitrogen bases generates strong broad ν_{OH} bands shifted to the 3200–2700 cm^{-1} wavenumber region where they can not be resolved due to overlapping with each other and other bands (vide infra).

The hydroxyl groups, linked to phosphorous, give band at 3665 cm^{-1}. The appearance of a negative band at 3665 cm^{-1} was

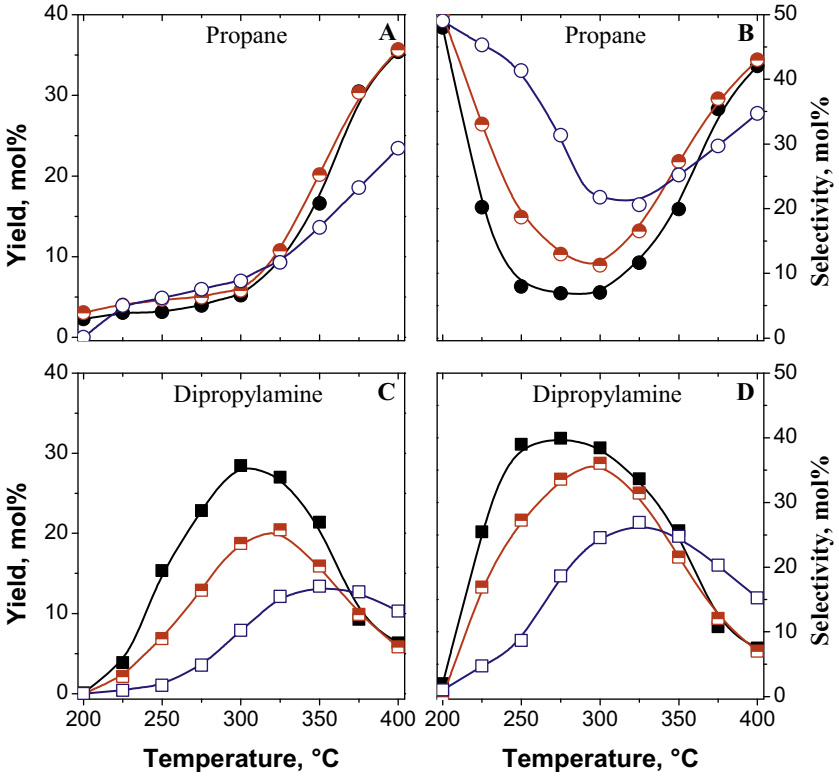

Fig. 7. Yields and selectivities of PA hydroconversion at H_2 partial pressures of 27.3 bar (full symbols), 40.5 bar (half-filled symbols), and 64.3 bar (empty symbols) as function of reaction temperature. The PA partial pressure and WHSV were 2.7 bar and 1 $g_{PA}\ g_{cat}^{-1}\ h^{-1}$, respectively.

found to be paralleled by the appearance of positive bands stemming from protonated nitrogen bases (vide infra). These finding suggests that, in contrast to silanol groups, the P-OH groups are acidic enough to donate protons to the strong nitrogen bases, present in the reacting gas (Fig. 8A, a).

The strong overlapping absorption bands around 3000 cm^{-1} can be attributed to asymmetric and symmetric $\nu(CH_3)$ and $\nu(CH_2)$ stretching vibrations of methyl and methylene groups of the adsorbed species. The corresponding deformation vibrations of the groups appear at

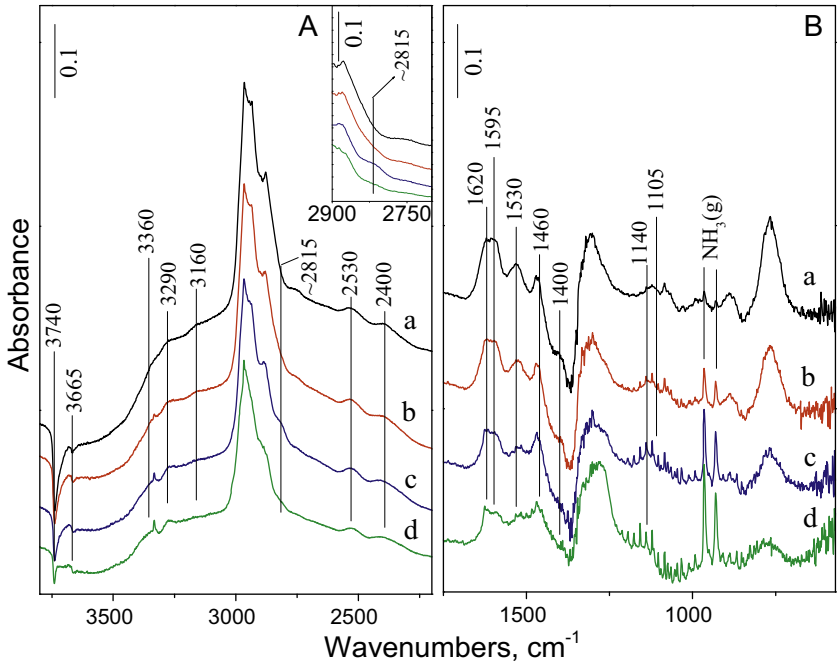

Fig. 8. Difference DRIFT spectra obtained from the reaction of PA/H_2 over Ni_2P/SiO_2 catalyst at (a) 250 °C, (b) 300 °C, (c) 350 °C, and (d) 400 °C. Hydrogen was passed through a PA-containing saturator, kept at 0 °C, at a flow rate of 30 $cm^3\ min^{-1}$. The partial pressure of PA and the total pressure were 0.14 bar and 20 bar, respectively. Each spectrum was obtained by subtracting the spectrum of the catalyst in H_2 from the corresponding spectrum of the catalyst and the reacting gas.

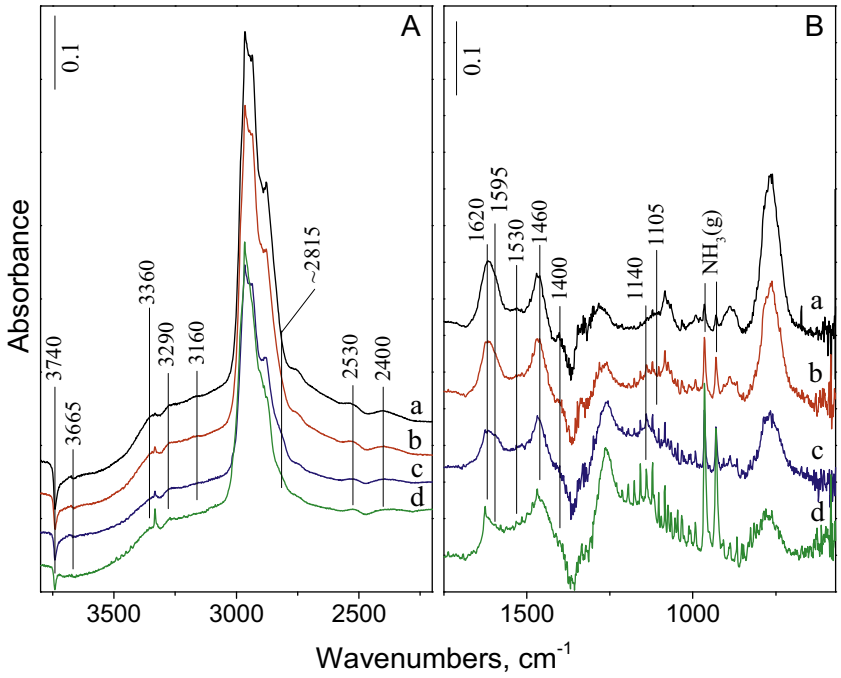

Fig. 9. Difference DRIFT spectra obtained from the reaction of PA/H_2 over Ni_2P/SBA-15 catalyst at (a) 250 °C, (b) 300 °C, (c) 350 °C, and (d) 400 °C. For further experimental conditions see the legend of Fig. 8.

1460 cm^{-1} ($\delta_{as}(CH_3)$, $\delta(CH_2)$) and 1400 cm^{-1} ($\delta_s(CH_3)$, $\omega(CH_2)$) [27–29].

The assignment of the bands of gaseous, adsorbed, and protonated N-bases, obtained from the HDN reaction is given in Table 2. Similar absorption bands at 3360, 3290, and 3160 cm^{-1} were observed before from the adsorption of ethylamine over WP/SiO_2 and assigned to protonated amine $C_2H_5NH_3^+$ [30]. However, from the adsorption of PA on surfaces not carrying Brønsted acid sites, such as silica or sodium zeolites, virtually the same absorption bands were obtained [29,31]. Latter results clearly show that these bands can not belong to protonated alkylamines. The bands at 3360 and 3290 cm^{-1} can be assigned to the $\nu_{as}(NH_2)$ and $\nu_s(NH_2)$ vibrations of the amine group of adsorbed primary amine, whereas the band at about 3160 cm^{-1} stems from the first overtone of the $\beta_s(NH_2)$ vibration mode having the frequency of 1595 cm^{-1} (Fig. 8B, a) [27,29]. Additional bands are discernible at about 1620 cm^{-1} on the high frequency side of the 1595 cm^{-1} band, and also a well separated band at 1530 cm^{-1}. The species obtained from adsorption of alkylamine over solid Brønsted acids gave similar bands, which were assigned as the $\delta_{as}(NH_3^+)$ and $\delta_s(NH_3^+)$ vibrations of the protonated amine [31–33]. The $\delta_s(NH_3^+)$ band at 1530 cm^{-1}, not overlapping with any other band, is particularly useful to follow the conversion of alkylamines to surface bound alkylammonium species. The $\nu(NH_3^+)$ band should appear as a strong broad band between 3200 and 2700 cm^{-1} [27,28]. The strong ν(OH) bands of silanol groups, which are H-bonded to nitrogen bases are shifted in the very same spectral region [34], generating a broad envelope of overlapping bands.

The absorption band at ~1105 cm^{-1} (Fig. 8B) can be assigned to the ν(C-N(H)) vibration of adsorbed PA [27,28]. When the reaction temperature was raised this band became weaker and new bands developed at about 2815 and 1140 cm^{-1} (Fig. 8A and B, b-d), corresponding to vibration frequencies of symmetric CH_2(N) and C–N(C) stretching vibrations, respectively [27,28]. Therefore, we attribute the appearance of these spectral features to DPA formed by PA disproportionation. The δ(NH) vibration of aliphatic secondary amines is generally very week, thus its contribution to the band observed around 1600 cm^{-1} must be negligible. Note that bands of DPA gain intensity as the reaction temperature is increased from 250 to 300 and 350 °C. However, at 400 °C the band becomes much weaker (Fig. 8A and inset). While dipropylamine disappears from the reaction system, bands of gas phase ammonia appear at 965–930 (inversion doubling), 1626 and 3334 cm^{-1} with rotational side bands. These results substantiate that DPA is intermediate of the PA HDN reaction, which is in full agreement with the catalytic results (Fig. 6).

A low intensity doublet at 2530 and 2400 cm^{-1} is also discernible in the spectra (Fig. 8A). Because similar bands were not obtained from adsorption of alkylamine over silica supports [29,31], it seems most probable that these bands stem from the $\nu_{as}(NH_2^+)$ and $\nu_s(NH_2^+)$ vibrations of protonated surface-bound

Table 2
Bands obtained from the HDN reaction of PA over silica-supported Ni_2P and Ni catalysts.[a]

Species	Frequency (cm^{-1}) (Vibrational mode)
Propylamine (PA)	3360 ($\nu_{as}(NH_2)$), 3290 (($\nu_s(NH_2)$), 3160 ($2 \times \beta_s(NH_2)$)[b], 1595 ($\beta_s(NH_2)$), **1105** **ν(C–N(H))**
Propylammonium ion (PAH^+)	3200–2700($\nu(NH_3^+)$)[c], 1620($\delta_{as}(NH_3^+)$), **1530** (**$\delta_s(NH_3^+)$**)
Dipropylamine (DPA)	**2815** (**$\nu_s(CH_2(N))$**), **1140** **ν(C–N(C))**, 1600 δ(NH)[d]
Dipropylammonium ion ($DPAH^+$)	**2530** (**$\nu_{as}(NH_2^+)$**), **2400** (**$\nu_s(NH_2^+)$**)
Ammonia (NH_3)	**3334** (**ν_s**(NH), **1626** (**δ_{as}(NH)**), **965–930** (**δ_s(NH)**)
Ammonium ion (NH_4^+)	3200–2900 ($\nu(NH_4^+)$)[b], 1500–1400 ($\delta(NH_4^+)$)[e]

[a] The bands given in bold are considered diagnostic regarding the catalytic PA HDN mechanism.
[b] First overtone of $\beta_s(NH_2)$ at 1595 cm^{-1}.
[c] Strong broad band overlapping with red shifted ν_{OH} bands.
[d] Very weak band hardly discernable due to overlapping with the strong ($\delta_{as}(NH_2)$) band.
[e] Broad band overlapping with CH deformation bands.

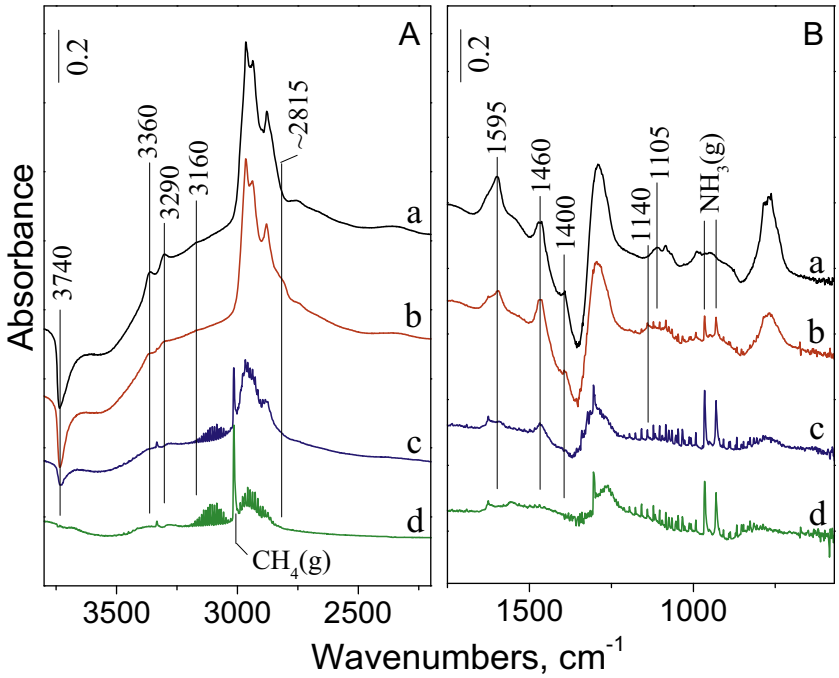

Fig. 10. Difference DRIFT spectra obtained from the reaction of PA/H_2 over Ni/SiO_2 catalyst at (a) 100 °C, (b) 200 °C, (c) 300 °C, and (d) 400 °C. For further experimental conditions see the legend of Fig. 8.

DPA [27,28]. These bands, together with the $\delta_s(NH_3^+)$ band of protonated PA (PAH^+) at 1530 cm^{-1} appear with lower intensity over the Ni_2P/SBA-15 catalyst (Fig. 9). This was accounted for the lower concentration of the P-OH related strong Brønsted acid sites in the latter sample. Indeed, the P-OH band of the Ni_2P/SBA-15 catalyst was weaker than that of the Ni_2P/SiO_2 catalyst (not shown).

The changing band intensity shows that the surface concentration of PAH^+ varies with the reaction temperature (Fig. 8). However, this surface concentration did not show any correlation with the concentration of the DPA. These results suggested that the PAH^+ species are spectator species in the DPA-forming reaction. In order to further clarify the role of strong Brønsted acid sites in the PA disproportionation reaction, Ni/SiO_2 catalyst, not having strong acid P-OH sites, was also investigated.

Infrared spectra of surface species formed from PA/H_2 mixture over Ni/SiO_2 catalyst are shown in Fig. 10. Because this catalyst was more active than the Ni_2P/silica catalyst (Fig. 6C) the first spectrum was recorded at temperature as low as 100 °C (Fig. 10, a). Virtually the same surface species were identified than over the silica-supported Ni_2P catalyst (cf. Figs. 8 and 10, spectra a) but, in absence of strong Brønsted acidity, no bands of PAH^+ appeared.

The bands of DPA and reaction product NH_3 appeared already at reaction temperature 200 °C (Fig. 10). Notice the bands at 2815 cm^{-1} ($\nu_s(CH_2(N))$ and 1140 cm^{-1} 1 (ν(C–N(C)) and the sharp bands of gas phase ammonia (Fig. 10, spectra b). At reaction temperatures 300 °C and above DPA started to become converted to gas phase hydrocarbon and ammonia (Fig. 10, b–d). At the highest reaction temperature (400 °C) the spectrum is dominated by the sharp vibration band of gas phase CH_4 at 3015 cm^{-1} and its rotational side bands. These spectral changes are in full agreement with the catalytic results and suggest that the HDN reaction of PA follows a similar pathway on the supported Ni catalyst than over the Ni_2P catalyst. However, the former catalyst shows high activity also in the hydrogenolysis of the C—C bonds leading to fragmentation of the hydrocarbon chain (cf. Figs. 10 and 6C).

4. Discussion

4.1. Catalyst topology

The strength of the C≡O bond and, as a consequence, the ν(CO) frequency of surface carbonyl species strongly depends on the chemical environment and the electronic state of the adsorption site. Provided that the kinds of carbonyls can be assigned to specific surface formations conclusions can be drown about the relative amounts of the different sorption sites. Together with TEM examinations the CO adsorption studies permit to draw conclusions about the topology of the catalyst surface.

The carbonyl band of the silica supported Ni_2P at 2195 cm^{-1} was assigned to weakly bound CO but the assignment of the species to specific adsorption sites remained a matter of discussion. Layman et al. [21,24] attributed a similar band to ν_{CO} vibration of a P═C═O species. In light of present results this assignment seems to be doubtful. Over the surface of the passivated Ni_2P/SiO_2 catalyst significant fraction of the surface Ni and P atoms are in an oxidation state of +2 and +5, respectively in Ni-phosphate-like species [8–10,21]. The band at 2195 cm^{-1} is stronger in the spectrum of this catalyst than in that of the H_2-activated catalyst (vide infra). In line with the finding of Busca et al. [19] we found that the modified silica, containing surface phosphate and hydrogen phosphate groups does not adsorb CO (Fig. 4B, f). These results substantiate that the band at 2195 cm^{-1} belongs to Ni^{2+}-CO species. This assignment is supported by earlier results of Hadjiivanov et al. [23].

Jensen et al. [25] shortly described the FT-IR spectra of CO adsorbed at room temperature on reduced Ni/SiO_2 catalyst. At CO pressure near to that applied in the present study bands were obtained from adsorption at 2067 and 1887 cm^{-1} assigned to terminal and bridging CO, respectively, bound to Ni metal particles. Moreover, bands appeared at 2035 and 2002 cm^{-1}, stemming from CO bound to defect sites of Ni particles and to the support, respectively. The higher ν(CO) frequency of the carbonyls, linearly bound to silica-supported Ni_2P catalyst (2090–2096 cm^{-1}, Fig. 4) compared to the corresponding frequency of the carbonyls bound to

Ni/silica (2067 cm^{-1}) catalyst was attributed to the electron withdrawing properties of the P atoms generating a minor positive charge on the Ni atoms ($Ni^{\delta+}$) [21,24]. Nevertheless, the Ni—P bond is covalent and the Ni_2P phase exhibit metallic character [8,24,35]. Despite the metallic character of Ni_2P no bridging carbonyl was formed over the Ni_2P/SiO_2. It was argued that the larger distance of surface nickel atoms in Ni_2P does not allow the formation of such species [22]. Unlike the carbonyls of the Ni/SiO_2 [25] the carbonyls of the Ni_2P/SiO_2, giving the bands at 2096 and 2035 cm^{-1}, resist flushing by He flow even at temperatures as high as 100 °C (Fig. 4A, c). Due to stronger π^* back-bonding carbonyls over surfaces of higher electron density have lower ν(CO) frequency, weaker C—O bond, than over surfaces of lower electron density, whereas the carbonyl groups bind stronger to sites of higher electron density [22,26,36]. Thus, the carbon monoxide bound to higher-energy sites of nickel, such as steps, kinks, corners, and edges, shows stretching mode with lower frequency than that adsorbed on terrace atoms [26]. The band at 2096 and 2035 cm^{-1} are assigned here to CO adsorbed on terrace atoms of crystal faces and on high-energy defect sites, respectively. The strong band at 2035 cm^{-1} (Fig. 4A) suggests that the Ni_2P particles of the fresh catalyst contain defect sites in high concentration. The small particles have rather disordered structure. Some of them may contain even residual nickel phosphate. It has to be noticed that adsorption on defect sites of Ni_2P particles not only gives a ν(CO) band shifted to lower wavenumbers but also produces ideal conditions to dipolar coupling interactions between the nearby carbonyl species of slightly different vibration frequencies. As a consequence the lower frequency species transfers intensity from its band to that of the higher frequency counterpart. This intensity transfer strengthens the 2096 cm^{-1} band of the terrace-bound CO promoting the detection of this species (Fig. 4A), however, makes the quantitative interpretation of the spectrum very difficult.

The carbonyl species giving band at 2035 cm^{-1} could not be detected at all over the Ni_2P catalysts, already used in HDN reaction (Fig. 4B,D). The absence of this band does not necessarily indicate the total absence of defect Ni_2P sites. As was pointed out by Hollins [36], just a few percent increase in the proportion of the high-frequency species was enough that the band of this species should dominate the infrared spectrum due to effect of dipolar coupling. It is obvious that the Ni_2P phase took up an ordered crystal form under reaction conditions (Fig. 2B). The particle size of the SiO_2 supported Ni_2P phase remained about the same, but the morphology changed from about globular particles, carrying virtually defect sites only, to particles with flat faces (Fig. 2A,B).

It follows from the above discussion that the Ni_2P/SBA-15 catalyst must contain less amorphous and defected Ni_2P particles and phosphate residue than the Ni_2P/SiO_2 catalyst (Fig. 4C). The CO species, having lower ν(CO) frequency, must be bound stronger than the species absorbing at higher frequency. The integrated intensity of both bands decreases when the CO coverage of the catalyst is decreased. In accordance with the strengths of adsorption the relative intensity loss of band at 2035 cm^{-1} is smaller than that of the band at 2096 cm^{-1} (Fig. 4, A and C). When the coverage is further decreased the high-frequency band is expected to disappear first and the low frequency band after. Interestingly, after disappearance of the low-frequency band a band remained at 2080 cm^{-1} (Fig. 4C). Similar ν(CO) band was obtained from the adsorption of CO over silica supported Ni catalysts [21,26]. The band at 2080 cm^{-1} suggests that a small fraction of the Ni precursor was reduced to Ni^0 even in the presence of excess amount of P precursor on the SBA-15 silica surface.

Because the Ni_2P particles were inside the narrow channels of the SBA-15 support, the pore size of the support somewhat limited the size and morphology change of the Ni_2P particles (Fig. 2C and D). A salient finding of the CO chemisorption and TEM study of the present work is that the structure and the surface of the working catalyst are quite different than that of the H_2 activated one. Interestingly, neither the CO chemisorption capacity nor the size of the Ni_2P particles in the activated and the used catalyst differs as drastically as the morphology of the particles.

The assignment of the band at 2055 cm^{-1} also raises questions (Fig. 4A,a; C,a). Both the silica supported Ni_2P and Ni catalysts were found to bind CO as species giving such infrared band. It was assigned first to volatile $Ni(CO)_4$ formed from CO and supported Ni and adsorbed on the support [23,24]. However, we do not believe that the similar band obtained from CO adsorption over Ni_2P/SiO_2 stems from adsorbed $Ni(CO)_4$. The formation of $Ni(CO)_4$ over Ni_2P must be strongly hindered [24]. The band at ~2055 cm^{-1} disappeared when the CO gas was flushed out from the DRIFTS cell by He flow. This event was paralleled by the strengthening of the bands at 2096 and 2035 cm^{-1} (Fig. 4A,a,b and C,a,b). Therefore we attribute the ~2055 cm^{-1} band to nickel subcarbonyl species $Ni(CO)_x$ ($x < 4$) that is transformed to monocarbonyl when the CO coverage of the surface is decreased.

Because it is important that the organic N-compound, such as the alkyl amine should bind near to the site where the H_2 is activated it was argued that at least a fraction of the P-OH groups must belong to the active hydrogenation phase to promote the interaction of the hydrogen and the nitrogen base [22,37]. It was suggested that the hydroxyl groups would come from phosphate species of the passivated catalyst that did not become fully reduced in the activation treatment by H_2. However, only a single kind of the P-OH group was detected on the surface of the Ni_2P/SiO_2 catalyst by DRIFT spectroscopy (Fig. 5). The ν(OH(P)) band was virtually the same strength regardless of the presence or absence of passivating phosphate-like surface layer on the Ni_2P particles. These results suggested that most of the P-OH groups come from silica-bound hydrogen phosphate and only a very small fraction of the surface P-OH groups may belong to the nickel-containing active phase. The carbonyl band at 2195 cm^{-1} (Fig. 4A), assigned to Ni^{2+}-CO, substantiates the presence of residual Ni^{2+} in the activated catalyst, however, we do not have information about the location of these nickel ions and evidence about the presence of P-OH near to the surface of Ni_2P particles.

Two kinds of Ni atoms are distinguished in the Ni_2P crystals regarding the number of the nearest coordinating P atoms, namely, four and five coordinated Ni atoms, designated as Ni(1) and Ni(2), respectively [38]. Both kinds of Ni atoms are present on the surface of the Ni_2P crystals but Ni(2) was shown to be the dominating surface Ni atom in the catalysts containing highly dispersed Ni_2P particles [38]. The present work clearly shows that the Ni_2P particles have a highly defected structure in their initial reduced state of the catalyst. This structure substantiates that the surface of the particles is covered predominantly by Ni atoms in low coordination. This structure, having high electron density nickel atoms, were quite stable in hydrogen at the temperature of the reaction, but was rapidly converted to ordered crystals in contact with the PA reactant. It is rather common that adsorption interaction at elevated temperature increases the mobility of the atoms on a solid surface and promotes reorganization of the surface structure. In other words the catalytically active surface ensembles are generated in the interaction of the reactant and the catalyst. This finding points out the significance of operando methods in catalysis research.

4.2. PA hydroconversion

The results shown in Fig. 6 suggest that at lower reaction temperatures propane and ammonia, as well as, DPA and ammonia are predominantly primary products, obtained from PA by C—N bond hydrogenolysis and PA disproportionation, respectively. As the temperature was increased the DPA yield decreased while the

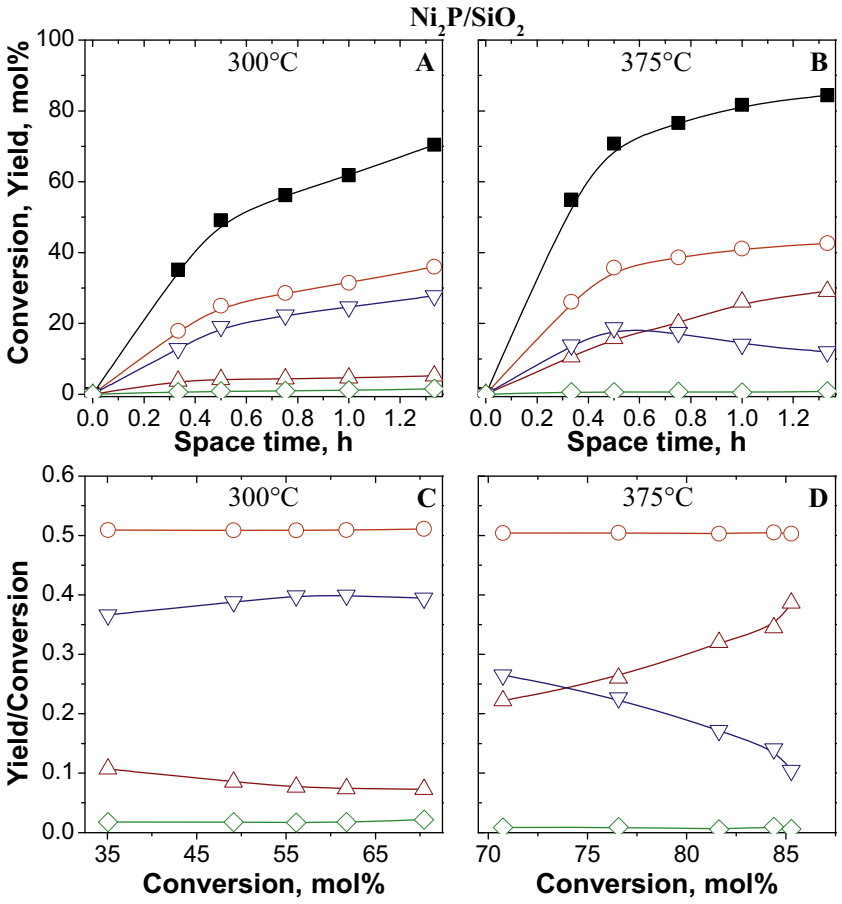

Fig. 11. Hydroconversion of PA (■) and yields of ammonia (○), propane (△), DPA (▽) and TPA (◊) as a function of the space time, and first rank Delplots of the products at 300 (A, C) and 375 °C (B, D). The PA and H_2 partial pressures were 2.7 and 27.3 bar, respectively.

propane yield increased at unchanged conversion. These results suggest that at higher temperatures the propane is formed mainly in consecutive reaction through hydrogenolysis of DPA intermediate. The PA disproportionation was studied by Geus et al. [39] over Ni/γ-Al_2O_3 catalyst at 5.6 kPa PA partial pressure and different H_2 partial pressures below 1 bar at 150 °C. In absence of hydrogen the catalyst was found to rapidly lose activity. In the presence of hydrogen DPA and ammonia were the only products. In line with the findings of Geus et al. [39] we found that increased hydrogen pressure suppressed the conversion of PA to DPA. This indicates that reaction of alkylamine HDN has complex chemistry. The effect of increased hydrogen pressure infers that disproportionation goes through an unsaturated intermediate, most probably through 1-propaneimine [39]. Thus, the dimerization can be described in steps of (i) PA dehydrogenation, (ii) acid catalyzed addition of PA to the obtained 1-propaneimine, (iii) the deammoniation of the thus obtained 2-amino dipropylamine to get the Schiff base propylidene propylamine, and finally (iv) the hydrogenation of the Schiff base to DPA. This outline of the process assumes that the catalyst is bifunctional, having both hydrogenation–dehydrogenation and Brønsted acid sites. This picture provides explanation for the finding that increased H_2 pressure suppressed the DPA formation over Ni_2P/silica catalysts by suppressing the dehydrogenation reaction.

$$CH_3CH_2CHNH_2 \Leftrightarrow CH_3CH_2CH{=}NH + H_2, \quad (1)$$

which reaction is the first step towards PA dimerization. This reaction also explains the temperature effect on the activity. At relatively low temperature the catalyst is able to activate hydrogen to break the C—N bond, however, the DPA formation and the conversion of PA remains low. Higher reaction temperatures shift the hydrogenation–dehydrogenation equilibrium in the direction of dehydrogenation. For instance, if the temperature is changed from 200 to 400 °C the equilibrium constant of Eq. (1) increases from 9×10^{-10} to 2×10^{-7}. In acid catalyzed reaction with PA the 1-propaneimine intermediate is rapidly consumed promoting further PA dehydrogenation and DPA formation. At about 275–350 °C the PA conversion reaches its maximum. The main product and the main surface species becomes the DPA. At higher temperatures again the hydrogenolysis of DPA and PA C—N bonds becomes the prevailing reaction, giving propane and ammonia.

It is important to note that no full conversion of PA could be reached on the Ni_2P catalysts (Figs. 6A,B), which might indicate equilibrium limitation. Reaction of propane with ammonia to form propylamine under applied conditions is very unlikely. However, in the presence of catalyst the addition of ammonia to propene is a facile reaction. The reaction is catalyzed either by acidic [40], basic [41] and metallic [42] active sites. The studied Ni_2P/silica catalytic system has both metallic hydrogenation/dehydrogenation activity and acidic properties. The propane must be in equilibrium with propane. This equilibrium favors propane especially at the high H_2 pressure and at the relatively low temperature of the HDN reaction. Nevertheless, the facile catalytic ammonia addition to olefin can establish a propane/propene/propylamine/ammonia equilibrium, where the propene concentration remains extremely low, but full propylamine conversion cannot be achieved, unless the catalyst is active in the HDN reaction but inactive in the reaction of ammonia addition to olefin.

The hydrogenolysis of the C—N bonds of PA results in propane and ammonia as primary products. The conversion of PA to DPA and TPA gives ammonia also as primary product and no propane. The propane obtained from the C–N hydrogenolysis of primary product DPA or TPA is secondary product. Thus, ammonia must be always primary product, whereas results suggest that propane can be formed both ways. It is primary product at low temperatures and secondary product at high temperatures. The analysis of conversion curves obtained at lower and higher temperature (Fig. 11A,B) was applied to support this statement. Extrapolation of selectivities to zero conversion, sometimes referred to as first-rank Delplot analysis [43,44], helps to distinguish primary and secondary products of complex reaction networks. Plot with non-zero intercept shows that the corresponding species is primary product. In accordance with above discussion the plots for ammonia (Fig. 11C,D) show that ammonia is primary product regardless of the reaction temperature. The Delplots of DPA also satisfy the criterion expected from a first rank product (Fig. 11C,D). In contrast, when the reaction temperature is increased, the intercept from propane changes as expected from finite to near zero indicating the rank alteration of the propane product.

No DPA was formed from PA over silica support but it was formed over both the Ni/SiO_2 and Ni_2P/SiO_2 catalysts. Neither the active phase nor the support of Ni/SiO_2 and Ni_2P/SiO_2 are the same. The Ni is distributed over a silica support, not having acid sites that were able to protonate even the strong base PA, whereas the Ni_2P is distributed over silica surface, carrying Brønsted acid P-OH groups, which were able to protonate N-bases. The active phases show hydrogenation/dehydrogenation activity and DPA is formed over both catalysts. The need for hydrogenation/dehydrogenation activity substantiates that DPA is formed through intermediate obtained by PA dehydrogenation, most probably through propaneimine. However, bands of propaneimine and protonated propaneimine could not be resolved from the complex operando DRIFT spectra, whereas the bands of DPA appeared. The surface concentration of the reaction intermediate propaneimine must be very low, because the equilibrium of Eq. (1) is shifted to the left at high H_2 pressure. The imine concentration is further decreased by its rapid conversion to DPA. Researchers often approach the problem of detecting intermediate by applying reaction conditions, which favor the formation of the intermediate and does not favor its conversion. It was possible to detect vibration bands of C=N– group at 1670 cm^{-1}, if we contacted the Ni_2P/SiO_2 catalyst with PA/He flow under reaction conditions. The corresponding DRIFTS spectra are shown in Fig. S3. It was claimed by Geus et al. [39] that beside dehydrogenation function Brønsted acid function is also needed to induce the addition of PA to 1-propaneimine. Interestingly DPA was generated also over non acidic Ni/SiO_2 catalyst. Results substantiate that Brønsted acid active sites are not necessary for the PA disproportionation and, therefore, probably play negligible role in the PA hydroconversion.

5. Conclusions

It is possible to obtain high yields of hydrocarbon and ammonia product from N-containing organic compounds, such as pyro-oil from animal by-products by catalytic HDN. The silica-supported nickel phosphide is active catalyst of the process. The reaction proceeds through secondary and tertiary amine intermediates. The results obtained with the model reactant propylamine suggest that formation of dipropylamine by-product can be suppressed and high conversion can be achieved at 350–400 °C reaction temperature and moderate (≤30 bar) H_2 partial pressures.

Acknowledgement

Thanks are due to the Hungary-Slovakia Cross-border Co-operation Program (Project registration number: HUSK/1101/1.2.1/0318) for supporting this research.

Appendix A. Supplementary data

Supplementary data associated with this article can be found, in the online version, at http://dx.doi.org/10.1016/j.apcatb.2014.09.001.

References

[1] E. Fumirsky, F.E. Massoth, Catal. Rev. 47 (2005) 297–489.
[2] S.T. Oyama, X. Wang, Y.-K. Lee, K. Bando, F.G. Requejo, J. Catal. 210 (2002) 207–217.
[3] T. Gott, S.T. Oyama, J. Catal. 263 (2009) 359–371.
[4] D.A. Bulushev, J.R.H. Ross, Catal. Today 171 (2011) 1–13.
[5] E. Cascarosa, G. Gea, J. Arauzo, Renewable Sustain. Energy Rev. 16 (2012) 942–957.
[6] M. Ayllón, M. Aznar, J.L. Sánchez, G. Gea, J. Arauzo, Chem. Eng. J. 121 (2006) 85–96.
[7] E. Cascarosa, I. Fonts, J.M. Mesa, J.L. Sánchez, J. Arauzo, Fuel Process. Technol. 92 (2011) 1954–1962.
[8] S.J. Sawhill, D.C. Phillips, M.E. Bussell, J. Catal. 215 (2003) 208–219.
[9] A. Infantes-Molina, J.A. Cecilia, B. Pawelec, J.L.G. Fierro, E. Rodriguez-Castellón, A. Jimenez-Lopez, Appl. Catal. A 390 (2010) 253–263.
[10] P. Bui, J.A. Cecilia, S.T. Oyama, A. Takagaki, A. Infantes-Molina, H. Zhao, D. Li, E. Rodríguez-Castellón, A.J. López, J. Catal. 294 (2012) 184–198.
[11] Y. Zhao, M. Xue, M. Cao, J. Shen, Appl. Catal. B 104 (2011) 229–233.
[12] Y. Shu, Y.-K. Lee, S.T. Oyama, J. Catal. 236 (2005) 112–121.
[13] Subramani Velu, K. Santosh, Gangwal, Solid State Ionics 177 (2006) 803–811.
[14] H.Y. Zhao, D. Li, P. Bui, S.T. Oyama, Appl. Catal. A 391 (2011) 305–310.
[15] J.A. Cecilia, A. Infantes-Molina, E. Rodríguez-Castellón, A. Jiménez-López, S.T. Oyama, Appl. Catal. B 136–137 (2013) 140–149.
[16] X. Wang, P. Clark, S.T. Oyama, J. Catal. 208 (2002) 321–331.
[17] F. Lónyi, A. Kovács, Á. Szegedi, J. Valyon, J. Phys. Chem. C 113 (2009) 10527–10540.
[18] T. Gerlach, F.-W. Schütze, M. Baerns, J. Catal. 185 (1999) 131–137.
[19] G. Busca, G. Ramis, V. Lorenzelli, P.F. Rossi, A.L. Ginestra, P. Patrono, Langmuir 5 (1989) 911–916.
[20] G. Ramis, P.F. Rossi, G. Busca, V. Lorenzelli, A.L. Ginestra, P. Patrono, Langmuir 5 (1989) 917–923.
[21] S.J. Sawhill, K.A. Layman, D.R. Van Wyk, M.H. Engelhard, C. Wang, M.E. Bussell, J. Catal. 231 (2005) 300–313.
[22] Y.-K. Lee, S.T. Oyama, J. Catal. 239 (2006) 376–389.
[23] K. Hadjiivanov, M. Mihaylov, D. Klissurski, P. Stefanov, N. Abadjieva, E. Vassileva, L. Mintchev, J. Catal. 185 (1999) 314–323.
[24] K.A. Layman, M.E. Bussell, J. Phys. Chem. B 108 (2004) 10930–10941.
[25] M.B. Jensen, S. Morandi, F. Prinetto, A.O. Sjåstad, U. Olsbye, G. Ghiotti, Catal. Today 197 (2012) 38–49.
[26] S. Morandi, M. Manzoli, F. Prinetto, G. Ghiotti, C. Gérardin, D. Kostadinova, D. Tichit, Microporous Mesoporous Mater. 147 (2012) 178–187.
[27] P. Larkin, Infrared and Raman Spectroscopy; Principles and Spectral Interpretation, Elsevier Inc., 2011, Ch. 6.
[28] S. Holly, P. Sohár, Infrared Spectroscopy, Műszaki Könyvkiadó, Budapest, 1968, Ch. 2 (in Hungarian).
[29] R. Schenkel, R. Olindo, J. Kornatowski, J.A. Lercher, Appl. Catal. A 307 (2006) 108–117.
[30] P. Clark, X. Wang, P. Deck, S.T. Oyama, J. Catal. 210 (2002) 116–126.
[31] T. Morimoto, J. Imai, M. Nagao, J. Phys. Chem. 78 (1974) 704–708.
[32] P.A. Jacobs, J.B. Uytterhoeven, J. Catal. 26 (1972) 175–190.
[33] A.K. Ghosh, G. Curthoys, J. Chem. Soc. FT1 80 (1984) 99–109.
[34] C. Pazé, S. Bordiga, C. Lamberti, M. Salvalaggio, A. Zecchina, J. Phys. Chem. B 101 (1997) 4740–4751.
[35] J.A. Rodriguez, J.-Y. Kim, J.C. Hanson, S.J. Sawhill, M.E. Bussell, J. Phys. Chem. B 107 (2003) 6276–6285.
[36] P. Hollins, Surf. Sci. Rep. 16 (1992) 51–94.
[37] S.T. Oyama, Y.-K. Lee, J. Phys. Chem. B 109 (2005) 2109–2119.
[38] S.T. Oyama, Y.-K. Lee, J. Catal. 258 (2008) 393–400.
[39] M.J.F.M. Verhaak, A.J. van Dillen, J.W. Geus, Appl. Catal. A 109 (1994) 263–275.
[40] M. Deeba, M.E. Ford, Zeolites 10 (1990) 794–797.
[41] M. Beller, C. Breindl, Chemosphere 43 (2001) 21–26.
[42] J.F. Knifton, Catal. Today 36 (1997) 305–310.
[43] N.A. Bhore, M.T. Klein, K.B. Bischoff, Ind. Eng. Chem. Res. 29 (1990) 313–316.
[44] M.T. Klein, Z. Hou, C. Bennett, Energy Fuels 26 (2012) 52–54.